ARTICLE

OBC
www.rsc.org/obc

Studies on pyridazine azide cyclisation reactions

Robin D. Allan,[a] Jeremy R. Greenwood,†[a] Trevor W. Hambley,[b] Jane R. Hanrahan,*[c] David E. Hibbs,[b] Samia Itani,[a] Hue W. Tran[a] and Peter Turner[c]

[a] *Adrien Albert Laboratory of Medicinal Chemistry, Department of Pharmacology, The University of Sydney, N.S.W. 2006, Australia. E-mail: r_allan@pharmacol.usyd.edu.au*

[b] *Centre for Heavy Metals Research, School of Chemistry, The University of Sydney, N.S.W. 2006, Australia*

[c] *Faculty of Pharmacy, The University of Sydney, N.S.W. 2006, Australia. E-mail: janeh@pharm.usyd.edu.au*

Received 12th December 2003, Accepted 5th April 2004
First published as an Advance Article on the web 19th May 2004

Reaction of sodium azide with 4-methyl-3,5,6-tribromopyridazine results in the formation of 3,5,6-triazide intermediate which could cyclise to give two possible bicyclic products while *ab initio* calculations show that the formation of a tricyclic compound is extremely energetically unfavourable. However, experimentally, only one major product is isolated. The structure of this unstable product has been conclusively established by X-ray crystallography as 3,5-diazido-4-methyl[1,5-*b*]tetrazolopyridazine confirming theoretical predictions.

Introduction

Quinoxazolinediones (Fig. 1) with electron-withdrawing phenyl ring substituents are well known as potent competitive antagonists of AMPA/kainate sensitive ionotropic glutamate receptors (GluRs). 6,7-Dinitroquinoxaline (DNQX) is the prototypical example, for which the X-ray crystal structure of a construct of the receptor–ligand complex has been solved.[1] The neutral azinedione motif shows the remarkable ability to mimic the zwitterionic α-amino acid of glutamate, while the nitro groups do not seem to make critical interactions with the receptor. We therefore reasoned that by exchanging the electron-withdrawing nitro substituents for ring nitrogens, the electronic and thus bioisosteric properties of quinoxolinediones could be retained, while at the same time retaining receptor antagonism or partial agonism.

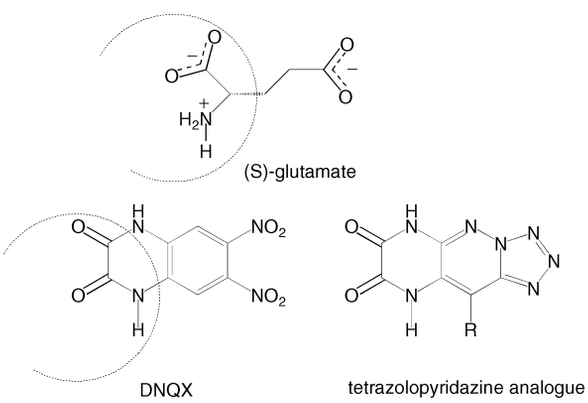

Fig. 1 (*S*)-glutamate, endogenous ligand for GluRs. DNQX presents a neutral α-amino acid bioisostere (ringed). The pyridazine analogue has similar electronic properties but altered steric properties.

Our strategy for developing the necessary chemistry to functionalise and cyclise pyridazine in the appropriate positions involved using sodium azide to replace ring halogens. This paper concerns the cyclisation, structure and tautomerism of the novel pyridazine azide intermediates formed.

Azide groups α-substituted to annular N-atoms in aromatic compounds are subject to tautomeric conversion to a tetrazole ring.[2] The potential energy surface on which this type of reaction takes place in solution has recently been investigated experimentally and theoretically.[3,4] It has been established for a series of 2,4-diazidopyrimidines and 4,6-diazidopyrimidines that the azido–tetrazole tautomerism is strongly solvent and temperature dependent and that the azide–azide and azide–tetrazole forms are energetically more favourable than the tetrazole–tetrazole form.[5] It has been proposed that the tetrazole–tetrazole form is disfavoured due to the charge distribution.[6] In the crystalline state, both 2,4-diazidopyrimidine[7] and 3,6-diazidopyridazine are found in the azide–tetrazole form.[6]

Reaction of isomeric 7-methyl- and 8-methyl-6-hydrazinotetrazolo[1,5*b*]pyridazines with nitrous acid is known to afford two stable isomeric methyl 6-azidotetrazolo[1,5-*b*]pyridazines. Furthermore, heating 6-azido-7-methyl-tetrazolo[1,5-*b*]pyridazine results in conversion to the thermodynamically more stable isomer, 6-azido-8-methyl-tetrazolo[1,5-*b*]pyridazine and a subsequent reduction to 6-amino-8-methyl-tetrazolo[1,5-*b*]-pyridazine.[8] Were the pyridazine triazides to follow this pattern, the 6,7-diazido-8-methyl-tetrazolo[1,5-*b*]pyridazine intermediate (**7**) would provide a route to the target analogues of DNQX.

Discussion

Reaction of citraconic acid anhydride (**1**) with bromine at room temperature for 1 week gave a high yield of *trans*- and *cis*-2,3-dibromo-2-methyl succinic anhydride which was subsequently converted to bromocitraconic anhydride (**2**) by treatment with pyridine in chloroform.[9] 5-Bromo-4-methyl-3,6 (1*H*,2*H*)-pyridazinedione (**3**) was prepared by modified procedures based on those of Coads *et al.*[10] and Vaccarella.[11] Reaction of (**3**) with phosphorus(v) oxybromide[12,13] yielded 3,5,6-tribromo-4-methylpyridazine (**4**) which gave the triazido intermediate (**5**) on reaction with excess sodium azide which subsequently cyclised. (Scheme 1).

Analysis by ^{1}H NMR spectroscopy of the product obtained from the reaction of 4-methyl-3,5,6-tribromopyridazine (**4**) with sodium azide indicated that only one product had been formed as determined by the presence of only one signal due to the methyl group. In the pyridazine series the generation of an azide group adjacent to a ring nitrogen results in immediate

† *Current address*: Department of Medicinal Chemistry, The Royal Danish School of Pharmacy, 2 Universitetsparken, DK-2100, Denmark.

DOI: 10.1039/b316190k

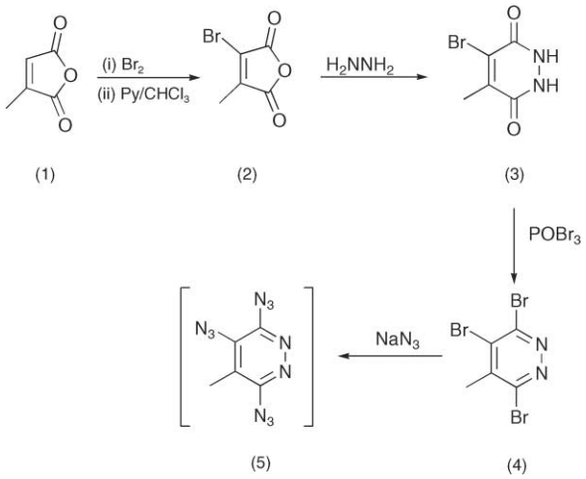

Scheme 1

cyclisation to stable tetrazolo[1,5-*b*]pyridazines.[8] In the case of the 3,5,6-triazidopyridazine intermediate (**5**), cyclisation could result in two possible bicyclic products (**6** or **7**) (Scheme 2). *Ab initio* calculations predicted that the formation of either of the two bicyclic products (**6** or **7**) is kinetically feasible, with a thermodynamic preference for **6**, while the formation of a tricyclic compound is energetically unfavourable (*q.v.*).

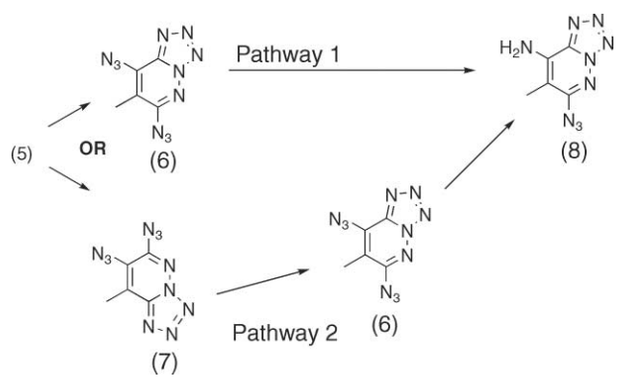

Scheme 2

Analysis of this product by mass spectrometry gave the molecular ion (MH^+) at *m*/*z* 218 in the mass spectrum. Although this molecular ion could result from either the triazido or a diazide–tetrazole product, the fragmentation patterns showed loss of N_2 (−28) followed by diprotonation of the resultant nitrene (+2) for two rather than three N_3 fragments [*m*/*z* 192 (51%) and 166 (36)]. This confirmed that the compound formed was diazidotetrazolo[1,5-*b*]pyridazine such as (**6**) or (**7**). No loss of a third N_2 was observed, this can be explained by the fact the tetrazolo ring is much more stable than azide. This is in accordance with the literature,[8,10] where 3,6-diazidopyridazines exist as azidotetrazolo[1,5-*b*]-pyridazines.

Structure determination

Initially, it was not possible to unequivocally determine which of the two isomeric products had formed. Heating of the product (**5**) resulted in the isolation of a single compound that was identified as 5-amino-3-diazido-4-methyl-tetrazolo[1,5-*b*]-pyridazine (**8**) (Scheme 2) by X-ray crystallography (Fig. 2). However, the precedent set by the isomerisation of 6-azido-7-methyl-tetrazolo[1,5-*b*]pyridazine to 6-azido-8-methyl-tetrazolo[1,5-*b*]pyridazine on heating meant that we were unable to conclusively identify the single product formed from the reaction of sodium azide with 4-methyl-3,5,6-tribromo-pyridazine (**4**).

Table 1 Bond distances (Å) and angles (°) with e.s.d.s in parentheses for Compound **8**

	Azo-amino-tetrazole (**8**)
N(1)–N(2)	1.357(3)
N(1)–C(4)	1.322(4)
N(2)–N(3)	1.307(3)
N(3)–N(4)	1.350(3)
N(4)–N(5)	1.340(3)
N(4)–C(4)	1.352(3)
N(5)–C(1)	1.317(3)
C(1)–C(2)	1.428(4)
C(2)–C(3)	1.372(4)
C(3)–C(4)	1.427(3)
N(6)–N(7)	1.256(3)
N(7)–N(8)	1.118(4)
C(1)–N(6)	1.407(4)
C(3)–N(9)	1.343(3)
C(2)–C(5)	1.504(4)
C(4)–N(1)–N(2)	105.6(2)
N(3)–N(2)–N(1)	111.5(2)
N(2)–N(3)–N(4)	105.8(2)
N(3)–N(4)–N(5)	122.7(2)
N(3)–N(4)–C(4)	108.5(2)
N(5)–N(4)–C(4)	128.8(2)
N(4)–N(5)–C(1)	111.4(2)
N(5)–C(1)–C(2)	127.5(3)
C(1)–C(2)–C(3)	117.7(2)
C(2)–C(3)–C(4)	116.5(2)
N(1)–C(4)–N(4)	108.6(2)
N(1)–C(4)–C(3)	133.3(2)
N(4)–C(4)–C(3)	118.0(2)
N(7)–N(6)–C(1)	113.0(2)
N(8)–N(7)–N(6)	172.4(4)

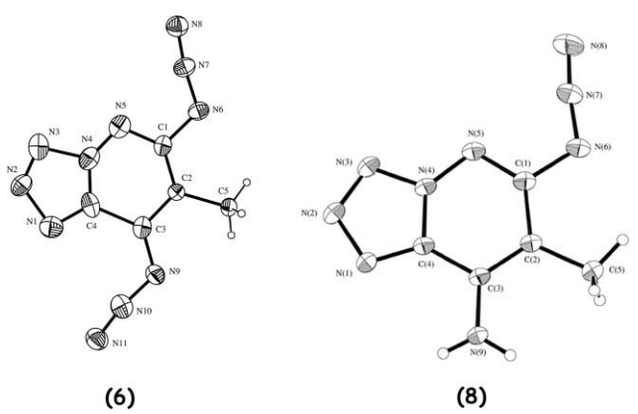

Fig. 2 Ortep representation of (**6**) and (**8**), ellipsoids shown at 60%.

This leaves two possible scenarios: either 3,5-diazido-4-methyl[1,5-*b*]tetrazolopyridazine (**6**) was produced and is directly reduced on heating to 5-amino-3-diazido-4-methyl-tetrazolo[1,5-*b*]pyridazine (**8**) (pathway 1), or 3,4-diazido-5-methyl[1,5-*b*]tetrazolopyridazine (**7**) was produced and undergoes rearrangement on heating to 3,5-diazido-4-methyl[1,5-*b*]-tetrazolopyridazine (**6**) and subsequent reduction to 5-amino-3-diazido-4-methyl-tetrazolo[1,5-*b*]pyridazine (**8**) (pathway 2), analogous to the methyl 6-azidotetrazolo[1,5-*b*]pyridazines.

All initial attempts to grow crystals of the unidentified compound (**6** or **7**) for X-ray diffraction resulted in twinned or otherwise unsuitable crystals that were prone to decomposition. Finally some very small crystals, unsuitable for diffraction using a standard radiation source but acceptable for a synchrotron radiation source were obtained. Although the structure was conclusively established to be 3,5-diazido-4-methyl[1,5-*b*]-tetrazolopyridazine (**6**) (Fig. 2) rather than the alternative (**7**), due to the highly mosaic nature of the crystal the data is not of sufficient quality to give precise structural parameters.

From Table 1, the N5–C1 and C2–C3 bond lengths of the pyridazine ring of (**8**) (1.317 and 1.372 Å) suggest an aromatic

character. This is in agreement with bond lengths of 6-azido-1,2,3,4-tetrazolo-[1,5-*b*]pyridazine.[7] Although azolopyridazines with a bridgehead N atom are considered to be fully aromatic 10π-electrons, in the crystal structure of tetrazolo[1,5-*b*]-pyridazine the corresponding bond lengths (1.298 and 1.353 Å) are indicative of double-bond character.[15]

The fusion of the tetrazole ring results in strong deformation of the pyridazine ring as has been described previously for related compounds.[7,15] The N5–N4–C4 angle (**8**) is 128.2° compared to 129° for the 6-azido-1,2,3,4-tetrazolo-[1,5-*b*]-pyridazine[15] and 128° for tetrazolo[1,5-*b*]pyridazine.[7] Additionally, the N4–N5–C1 bond of 8 (111.4 Å) is in accordance with the values published for 6-azido-1,2,3,4-tetrazolo-[1,5-*b*]-pyridazine and tetrazolo[1,5-*b*]pyridazine (111 and 112.5°) respectively.[7,15]

The N–N–N bond angle of the azide groups in compound (**8**) departs from 180° by 8° (Table 1) which is characteristic for azide goups[7] and can be attributed to the contribution of the third mesomeric form of the azide resonance structure, $–N=N^+=N^- \leftrightarrow –N^-–N^+\equiv N \leftrightarrow –N^+\equiv N^+–N^{2-}$. The C1–N6 bonds of (**8**) is characteristic for single bonds which indicates no or only a marginal contribution of the mesomeric form with the negative charge transferred to the pyridazine ring, which is in agreement with the structure of 6-azido-1,2,3,4-tetrazolo-[1,5-*b*]pyridazine.[7] However, the C3–N9 bond length of (**8**) suggests double bond character indicating some delocalisation of the negative charge to the pyridazine ring may be present.

The angle between the pyridazine and tetrazole rings for **8** does not differ significantly from zero (N2–N3–N4–N5, 0.4°), which is in agreement with the torsion angle for tetrazolo-[1,5-*b*]pyridazine (0.8°).[15]

Ab initio calculations

The cyclisation reactions of methylpyridazine diazides (Scheme 3) and triazides (Scheme 4) were studied using hybrid density functional theory (B3LYP/6-311+G(d,p)), and complete basis set treatments (CBS–4M).[16] Minima and transition states were characterised by frequency analysis, and solvation was considered *via* a Poisson–Boltzman self-consistent reaction field (PB-SCRF).[17] For the transition states in solution, optimisation proved intractable using this model. The cyclisations are summarised in Schemes 3 and 4 with transition states in light grey, and the energies given in Table 2 with transition states in *italics.* All calculations agree that in all phases, for the diazide the 5-methyl bicyclic (**12**) form is slightly favoured over the 4-methyl form (**11**) (Scheme 3). For the triazide however,

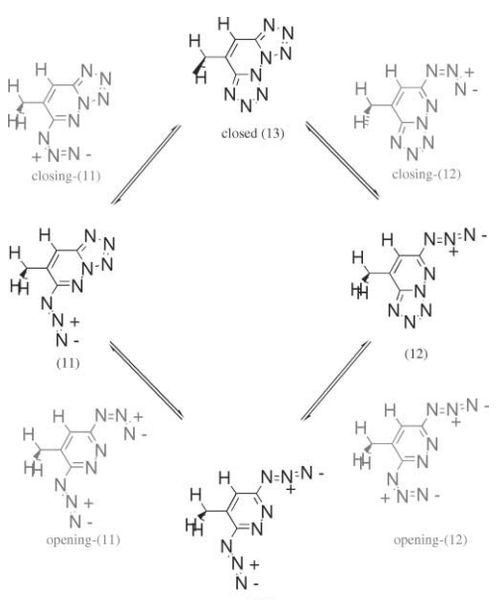

Scheme 3

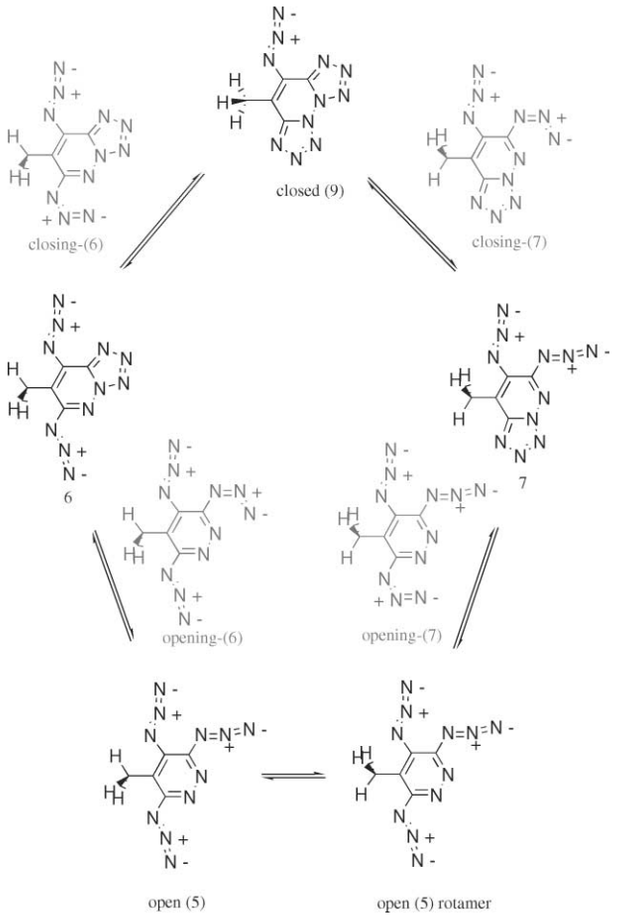

Scheme 4

the 4-methyl bicyclic form (**6**) (Scheme 4) is universally favoured. Additionally, bicyclic forms {(**6**), (**7**), (**11**), (**12**)} are consistently more stable than monocyclic {open (**5**), open (**10**)} or tricyclic {closed (**9**), closed (**13**)} forms. This is in full qualitative agreement with the available experimental evidence for cyclisation of the diazide[7,14] and with the current findings regarding the triazide. The optimised geometries are also broadly consistent with the X-ray structures, and the reaction path follows closely that described by Cubero *et al.*[3] According to the PB-SCRF continuum solvation model, the solvent has some effect on the equilibrium between the bicyclic products for both diazide and triazide. Whereas in gas phase, the energies of the bicyclic forms are predicted to differ by around 2 kcal mol^{-1} in favour of (**12**) and (**6**) over (**11**) and (**7**), this difference reduces with the polarity of the solvent to around 1 kcal mol^{-1}. One might therefore expect to be able to observe traces of the non-favoured isomer in the reaction mixture, depending on the solvent, however the slight differences between the solvation energies in THF and DMSO indicate that the precise solvation mixture of these two used experimentally is not a critical thermodynamic determinant of the reaction outcome. We note that continuum solvation models are generally not designed to treat solvent mixtures and rather than interpolate dielectric constant, density and solvent radius, we have studied the reaction in neat solvents.

The published NMR-based experimental measurement of the isomerisation energy of the diazide (**12**) in hot DMSO gives a difference of 5.9 kcal mol^{-1} *vs.* the isomer (**11**)[7] which is significantly greater than that calculated by any method here. However, the estimate was made on the basis of only two measurements separated by 5 °C. On the other hand, the kinetic measurement of an activation energy of 20 kcal mol^{-1} [7] is consistent with the gas phase barrier height according to B3LYP.

What remains unclear from either the calculations or the experiments is how much higher in energy the monocyclic

Table 2 Theoretical energies, relative energies and Gibbs free energies for potential intermediates and final products depicted in Schemes 3 and 4.

Phase		Gas phase								H_2O	THF	DMSO	Gas phase			H_2O	THF	DMSO
Component		E	E_{rel}	E+ZPE (0K)	E_{rel}	ZPE	ΔG_{298} (therm)	E+ZPE (0K)	E rel	ΔG_{solv} (PB–SCRF)			E (0K)	E_{rel}	G_{rel} (298K)			
Units		Hartree	kcal mol^{-1}	Hartree	kcal mol^{-1}	Hartree			kcal mol^{-1}				Hartree	kcal mol^{-1}				
Method	[b]	[a]		[b]				[c]		[b]			[d]		[e]			
Species[f]	**Symmetry**																	
Diazide																		
open (10)	C_s	−623.46391	6.7	−630.85513	2.9	0.10924	0.07133	−630.91955	2.7	−10.4	−8.8	−10.8	−629.93495	9.9	8.9	11.2	14.1	15
opening-(11)		*−623.43112*	*27.2*	*−630.82484*	*21.9*	*0.10845*	*0.07192*	*−630.88824*	*22.3*				*−629.90313*	*29.8*	*29.8*			
(11)	C_s	−623.47190	1.6	−630.85658	2.0	0.11141	0.07537	−630.92066	2.0	−12.7	−13.2	−16.5	−629.94793	1.7	1.9	0.8	1.4	1.1
closing-(11)		*−623.42967*	*28.1*	*−630.81701*	*26.8*	*0.11003*	*0.07501*	*−630.88040*	*27.3*				*−629.91060*	*25.1*	*26.1*			
closed (13)	C_1	−623.45525	12.1	−630.83663	14.5	0.11172	0.07613	−630.90058	14.6	−15.2	−14.6	−17.9	−629.94022	6.5	7.5	3.1	4.9	4.6
closing-(12)		*−623.43138*	*27.1*	*−630.81859*	*25.8*	*0.11004*	*0.07491*	*−630.88204*	*26.2*				*−629.91217*	*24.1*	*25.0*			
(12)	**C_s**	**−623.47453**	**0.0**	**−630.85978**	**0.0**	**0.11141**	**0.07515**	**−630.92385**	**0.0**	**−11.8**	**−13.0**	**−15.9**	**−629.95064**	**0.0**	**0.0**	**0.0**	**0.0**	**0.0**
opening-(12)		*−623.43173*	*26.9*	*−630.82606*	*21.2*	*0.10845*	*0.07185*	*−630.88940*	*21.6*				*−629.90407*	*29.2*	*29*			
Triazide																		
open (5)	C_1	−785.19159	7.5	−794.47916	2.7	0.11188	0.06832	−794.56040	2.7	−11.5	−8.8	−10.9	−793.32870	9.0	7.6	12.3	12.3	13.2
opening-(6)		*−785.16102*	*26.7*	*−794.45095*	*20.4*	*0.11115*	*0.06966*						*−793.29812*	*28.2*	*27.8*			
(6)	**C_s**	**−785.20350**	**0.0**	**−794.48354**	**0.0**	**0.11417**	**0.07367**	**−794.56479**	**0.0**	**−14.7**	**−12.1**	**−15.0**	**−793.34308**	**0.0**	**0.0**	**0.0**	**0.0**	**0.0**
closing-(6)		*−785.16034*	*27.1*	*−794.44249*	*25.8*	*0.11259*	*0.07252*						*−793.30400*	*24.5*	*25.1*			
closed (9)	C_1	−785.1827	13.1	−794.45961	15.0	0.11458	0.07447	−794.54078	15.0	−12.8	−13.3	−16.7	−793.33104	7.6	7.9	9.5	6.3	5.9
closing-(7)		*−785.15682*	*29.3*	*−794.44129*	*26.5*	*0.11243*	*0.07174*						*−793.30225*	*25.6*	*25.1*			
(7)	C_1	−785.19766	3.7	−794.48026	2.1	0.11381	0.07164	−794.56124	2.2	−15.6	−12.9	−16.0	−793.33983	2.0	1.3	1.1	1.2	1.1
opening-(7)		*−785.15864*	*28.2*	*−794.44867*	*21.9*	*0.11109*	*0.06911*						*−793.29621*	*29.4*	*28.9*			
open (5) rot.	C_s	−785.19150	7.5	−794.47909	2.8	0.1119	0.0683	−794.56033	2.8	−11.4	−8.3	−10.7	−793.32892	8.9	7.5	12.3	12.7	13.2

[a] HF/3-21G [b] B3LYP/6-311+G(d,p) [c] B3LYP/aug-cc-pVTZ + ZPE (B3LYP/6-311+G(d,p)) [d] CBS–4M [e] CBS–4M + PB–SCRF (B3LYP/6-311+G(d,p)) [f] Open: monocyclic. Closed: tricyclic. Number alone: bicyclic. *Italics*: transition state (opening – bicyclic to monocyclic, tetrazole to azide; closing – bicyclic to tricyclic, azide to tetrazole; see Schemes 3, 4). Normal text: local minimum. **Bold**: lowest energy form. Rot.: methyl group rotamer.

(open) and tricyclic (closed) forms are than the bicyclic forms, nor indeed whether the monocylic {diazide open (**10**), triazide open (**5**)} or tricylic {diazide closed (**13**), triazide closed (**9**)} form is least stable. B3LYP gives the tricyclic forms {(**13**), (**9**)} as 11–12 kcal mol^{-1} higher in energy than the monocyclic forms {(**10**), (**5**)}, while CBS–4M predicts that the tricyclic forms are more stable by about 3 kcal mol^{-1}. Also, relative to the favoured bicyclics, the stabilities of these forms are predicted to be strongly dependent on the solvent. Thus, while solvation has modest influence on the product distribution, it has a profound effect on the cyclisation thermodynamics. A similar situation arises for the well-studied analogous tautomerism of maleic hydrazide, where the pyridazine nitrogens are most stable when differently hybridised (sp_2,sp_3) but the question of whether (sp_2,sp_2) or (sp_3,sp_3) is least stable is more difficult to answer.[18] Analogy with the tautomeric preference of maleic hydrazide would make the tricyclic (sp_3,sp_3) forms least stable, in accordance with the B3LYP results obtained in this study.

Use of sufficiently large basis sets are known to be especially important when comparing nitrogen-containing heterocycles with varying heteroatom hybridisation.[19] The sufficiency of the 6-311+G(d,p) basis set for treating these compounds was confirmed by comparison with B3LYP optimisation of key species using the larger correlation consistent basis set, aug-cc-pVTZ; differences in relative energies were on the order of 0.2 kcal mol^{-1}, indicating that the results here are close to the basis set limit for B3LYP. However, we recently noted substantial (3 kcal mol^{-1}) deviations between the basis set limit for B3LYP calculations and G2 or CBS–QB3 energies for another case involving isomeric heterocycles.[20] Even at the basis set limit, B3LYP struggles to achieve chemical accuracy for questions of heteroaromatic tautomerism and isomerism.

It is also noteworthy that the low barrier to rotation of the aromatic methyl group leads to low frequency vibrations and complicates the thermochemical analysis. While the CBS–4M method treats electron correlation at the MP4 level and with complete basis set extrapolation at the MP2 level, it suffers from geometry calculated at HF/3-21G. The N–N distances in particular are poorly reproduced by HF/3-21G; differences up to 0.05 Å are noted between this level and B3LYP/6-311+G(d,p). The poor crystal quality and instability of the 3,5-diazido-4-methyl[1,5-*b*]tetrazolopyridazine resulted in crystal structure data for this structure that is not sufficiently accurate enough for quantitative comparison, however, the DFT N–N bond lengths are substantially closer to the comparable experimental bond lengths of the 5-amino derivative (RMS = 0.005 *vs*. 0.029 for 6 N–N distances). In the absence of higher level calculations (MP4 or CCSD(T) with a larger basis set, currently prohibitively expensive for this systems of this size) the DFT calculations are probably the more reliable of the two methods trialled here.

The results indicate that very high levels of *ab initio* theory and large basis sets are necessary for obtaining a consistent picture of heterocyclic systems in which the hybridisation of the heteroatoms varies between isomers. Azides are also problematic for this type of continuum solvation calculation, in particular for transition states, since Jaguar[17] uses Lewis dot structures for assigning atom types and thus the atomic radii used to determine the molecular cavity; multiple resonance forms lead to several possible assignments of atom radii when determining the molecular cavity. The systems examined here present a greater challenge for *ab initio* calculations than the majority of medium-sized uncharged ground-state organic molecules.

Conclusion

Unlike the diazide (**10**) which cyclises to (**12**) giving a route to functionalised 5-methyltetrazolo[1,5-*b*]pyridazines, the triazide (**5**) cyclises to (**6**) giving a synthetic route to functionalised 6-methyltetrazolo[1,5-*b*]pyridazines. This behaviour is consistent with the thermodynamics of the cyclisation reaction, as described here theoretically. Such tetrazolopyridazines may prove to be a useful addition to the medicinal chemist's toolbox, for example as replacements for nitroaromatics, which are often disfavoured for toxicological reasons.

Computational methods

All structures were optimised at RHF/3-21G and B3LYP/6-311+G(d,p) in Gaussian 98 rev. A7.[21] Transition states were located by QST2 or QST3 methods. Tight SCF convergence was used throughout, and ultrafine grids were used for B3LYP calculations. Minima and transition states were characterised and thermochemistry analysed by frequency analysis, with reoptimisation using tight criteria and symmetry where necessary. Alternative rotamers were considered; only 3,5,6-triazido-4-methylpyridazine displayed two rotameric minima about the methyl group. Compound method CBS–4M gas phase energies were calculated for the minima at the RHF/3-21G geometries, as per definition.[16] CBS–4M energies for the transition states were calculated at the frozen RHF/3-21G geometries. All minima were reoptimised at B3LYP/6-311+G(d,p) using Jaguar 4.1,[17] in gas phase and with three types of solvation (PB-SCRF continuum model): default = water (ε = 80.37, probe radius = 1.40), DMSO (ε = 45, probe radius = 2.41463), and THF (ε = 7.52, probe radius = 2.52361). Analytic SCF (ultrafine) and fine grid for B3LYP were specified (*NB* absolute B3LYP energies differed between Gaussian and Jaguar, but relative energies differed by less than 0.1 kcal mol^{-1}). Cavitation energy and surface area terms are omitted by default for THF and DMSO. The free energies of solvation were calculated as the differences between the energies of the optimised structures in solution and in the gas phase according to Jaguar, and added to the CBS–4M energies to give total and relative energies in solution (Table 2).

Experimental

Melting points were determined using a Reichert hot-stage melting point apparatus and are uncorrected. ^{1}H NMR spectra were recorded at 300 MHz using a Varian Gemini 300 spectrometer. Chemical shifts (δ_H) are quoted in parts per million (ppm), referenced internally to tetramethylsilane (TMS) at 0 ppm. Low resolution mass spectra were recorded on a Finnigan/MAT TSQ 7000 LCMS/MS spectrometer; only molecular ions (M^+ or MH^+) and major peaks are reported with intensities quoted as percentages of the base peak. High resolution mass spectra were recorded on a Micromass QT of II; in the Department of Chemistry at the University of Wollongong; all samples were run using electrospray ionisation (ESI) with ions measured as protonated molecular ions (MH^+). Thin layer chromatography (TLC) was performed on Merck aluminium backed plates pre-coated with silica (0.2 mm, $60F_{254}$) which were developed using UV fluorescence (254 nm). Flash vacuum chromatography[22] was performed on silica gel (Merck silica gel 60, column grade, particle size 70–230 mesh). Elemental analyses (C, H, and N) were within +0.3% of the theoretical values and obtained by the J.E.A.F. (Department of Chemical Engineering, the University of Sydney). Chemicals were purchased from Aldrich at the highest available grade. THF was distilled under nitrogen from sodium-benzophenone. All reported yields have not been optimised.

Bromocitraconic anhydride (2) (3-bromo-4-methylmaleic anhydride)

A mixture of citraconic acid anhydride (**1**) (112.08 g, 1 mol) and bromine (176.7 g, 1.1 mol), in a stoppered 500 ml flask, was standing at room temperature (rt) for a week, monitored by ^{1}H

NMR. The excess bromine was removed by bubbling nitrogen through the reaction mixture in a well ventilated hood, followed by evaporation under reduced pressure until the clear mixture was only slightly red. ^{1}H nmr. of the crude product showed that this was a 50:1 mixture of adduct and starting material (by their olefinic signals). The product (271g, 99.6%) was a mixture of *trans*- and *cis*- 2,3-dibromo-2-methyl succinic anhydride. ^{1}H NMR δ 5.03 and 4.90 (total 1 H, C*H*Br), 2.19 and 2.10 (total 3 H, CH_3). To this crude adduct (271 g, 1 mol) in chloroform (500 ml), cooled in an ice bath, was added pyridine (79.12 g, 1 mol), dropwise over a period of 40 min, with the internal temperature maintained below 20 °C throughout the addition. The resulting clear reaction mixture was stirred at room temperature for *ca*. 1 h, monitored by ^{1}H NMR, until the reaction was completed. It was washed with water (3 × 140 ml), dried over Na_2SO_4. Removal of solvent under reduced pressure gave a crude product, bromocitraconic anhydride (**2**), as a solid (165.54 g, yield 86.7%). ^{1}H NMR δ 2.17 (s, CH_3). This crude product was used in the next step without further purification.

5-Bromo-4-methyl-3,6-(1*H*,2*H*)-pyridazinedione (3)

A slurry of hydrazine sulfate (112.8 g, 867 mmol) in distilled water (660 ml) was heated with stirring (external heat not exceeding 100 °C). The crude bromocitraconic anhydride (**2**) (165.54 g, 867 mmol) was added to the hot slurry of hydrazine sulfate in water and the reaction mixture was heated with efficient stirring (external heat not exceeding 100 °C) for 12 h (foaming). Hydrobromic acid (48% solution, 37.2 ml) was added and the reaction mixture was heated further for 2 h, then cooled down to rt. The solid was filtered, dried under reduced pressure for 1 h, then air-dried over the weekend (160.5 g). This solid was stirred in chloroform (400 ml) for 1 h to remove by-products. The remaining solid was filtered and dried at room temperature overnight (152.8 g, yield 86.0%). This crude product was used without further purification. An analytical sample of (**3**) was prepared by recrystallisation from methanol to give a solid (needles), mp 260–265 °C dec. ^{1}H NMR ($CDCl_3$/d_6-DMSO) δ 2.25 (s, CH_3). MS (CI, CH_4) *m*/*z* 207.1 (100%) (MH^+ + 2), 207.1 (100%), 205.1 (99) (MH^+); (ESI) 204.9619 (MH^+ − $C_5H_6N_2O_2Br$ requires 204.9613).

3,5,6-Tribromo-4-methylpyridazine (4)

In a 2-necked 250 ml round bottom flask, equipped with a magnetic stirring bar, a reflux condenser with a P_2O_5 drying tube and a thermometer, a mixture of phosphorus(v) oxybromide[6,7] (112.2 g, 0.39 mol, 2.8 equiv.) and 5-bromo-4-methyl-3,6-(1*H*,2*H*)-pyridazinedione (**3**) (28.4 g, 0.14 mol) was heated for 0.5 h with external heat not exceeding 60 °C. The mixture turned into a slurry and went into a dough-like yellowish solid. It was then further heated at 100 °C (external heat not exceeding 100 °C) for 3 h (internal temperature was *ca*. 77 °C) during which time the reaction mixture turned into a solid mass. This solid mass was cooled down to room temperature over 3 h, broken up to slightly lumpy powder with a sturdy spatula, taking care to exclude moisture. The work-up involved a careful addition of this powder (portion wise) into a carefully maintained, vigorously stirred mixture of ice (100 g), CH_2Cl_2 (800 ml) and concentrated 28% ammonia solution (added portion wise to maintain the basic pH, a total volume of 250 ml was used). Keeping the pH basic (8 or higher) and the internal temperature below 5 °C throughout the work-up (*ca.* 1 h) avoided unwanted hydrolysis of the product. Removal of an insoluble gelatinous material by filtration allowed the separation of the organic layer. The dichloromethane extract was washed with water, dried over anhydrous Na_2SO_4, concentrated under reduced pressure to yield (**4**) as a powder (25.8 g, total yield 56.0%), mp 150–151 °C. ^{1}H NMR ($CDCl_3$, TMS) δ 2.69 (s, CH_3); (CI, CH_3) *m*/*z* 335 [(MH^+ + 6), 33.1%], 333 [(MH^+ + 4), 94.9], 331 [(MH^+ + 2), 100.0], 329 (MH^+, 37.6), 257 (19.1), 255 (21.6), 253 (33.8), 251 (17.2), 175 (3.2), 173 (82.8), 171 (77.7) (Found: C, 18.09; H, 1.01; N, 8.41. $C_5H_3Br_3N_2$ requires C, 18.15; H, 0.91; N, 8.47%).

3,5-Diazido-4-methyl[1,5-*b*]tetrazolopyridazine (6)

To a solution of 4-methyl-3,5,6-tribromopyridazine (**4**) (1.0 g, 3.02 mmol) in a mixed solvent (6 ml THF and 3 ml DMSO) at room temperature (18 °C) was added sodium azide (884 mg, 13.6 mmol). NaN_3 was initially almost completely soluble but soon after the addition, a white precipitate was formed. The reaction mixture became coloured (orange) about 10 min after addition. It was stirred at room temperature and monitored by ^{1}H NMR for *ca*. 7 h. Volatile solvent was removed under reduced pressure. The crude reaction mixture was taken up in ethyl acetate (90 ml), washed in turn with water (3 × 10 ml), brine (10 ml), dried over anhydrous Na_2SO_4 and concentrated under reduced pressure until dryness. Purification by chromatography (5% ethyl acetate/95% hexane) and subsequent crystallisation afforded the potentially explosive title compound as a solid (296 mg, yield 45%). An analytical sample of this compound was prepared by recrystallisation from ethyl acetate and hexane to yield a twinned solid, mp 131–132 °C (Found: C, 27.80; H, 1.45; N, 70.71. $C_5H_3N_{11}$ requires C, 27.66; H, 1.39; N, 70.95%). ^{1}H NMR (300 MHz, $CDCl_3$) δ 2.205 (s, CH_3). (CI, CH_3) *m*/*z* 218 (MH^+, 100.0%), 192 (51), 190 (13.5), 166 (36).

5-Amino-3-azido-4-methyl-[1,5-*b*]-tetrazolopyridazine (8)

A solution of diazidotetrazolo[1,5-*b*]pyridazine (**6**) (35.0 mg, 0.16 mmol), in hot toluene (3 ml, AR grade) was refluxed for 18 h and monitored by TLC until disappearance of the starting material. The toluene was removed under reduced pressure to give a solid residue. The crude product was taken up in chloroform. Purification by chromatography ($CHCl_3$) and subsequent crystallisation afforded a yellow solid (9.6 mg, yield 31.2%). An analytical sample of this compound was prepared by recrystallisation from EtOAc to yield twinned crystals, mp 227.0–227.5 °C dec. (darkening from 170 °C) (Found: C, 31.67; H, 2.76; N, 65.69. $C_5H_5N_9$ requires C, 31.42; H, 2.64; N, 65.95%). ^{1}H NMR (300 MHz, $CDCl_3$, TMS) δ 5.6 (bs, NH_2), 2.133 (s, CH_3). (CI, CH_3) *m*/*z* 192 (MH^+, 100.0%), 166 (28).

Crystal structures ‡

3,5-Diazido-4-methyl[1,5-*b*]tetrazolopyridazine (6)

The single crystals obtained for (**6**) were too small to provide an acceptable data set from a conventional laboratory diffractometer. Data were obtained during commissioning studies at the ChemMatCARS facility at the Advanced Photon Source of the Argonne National Laboratory, Argonne USA. Double diamond (111) reflections were used to obtain monochromated 0.56356 Å radiation from the synchrotron source, and harmonics were eliminated with mirrors. A colourless prismatic crystal of formula $C_5H_3N_{11}$ grown from a saturated solution in ethyl acetate and hexane at ambient temperature; Monoclinic, a = 8.124(4), b = 16.606(10), c = 7.179(3) Å, α = 90, β = 113.24(2), γ = 908, space group *P*21/*n*, U = 889.9(7) Å^3, Z = 4, D_c = 1.621 mgm^{-3} was attached with Exxon Paratone N, to a short length of fibre supported on a thin piece of copper wire inserted in a copper mounting pin. The pin and crystal were mounted on a unique Bruker Kappa diffractometer equipped with a with 4 chip mosaic CCD detector, and an Oxford Scientific Cryojet. Data were collected at 150(2) Kelvin with ϕ scans to 39.2 ° 2θ, and cell constants were obtained from a least squares refinement against 1478 reflections located between 4 and 39° 2θ R = 0.2333.

‡ CCDC reference numbers 227308 and 231327. See http://www.rsc.org/suppdata/ob/b3/b316190k/ for crystallographic data in.cif or other electronic format.

5-Amino-3-azido-4-methyl-[1,5-*b*]-tetrazolopyridazine (8)

A pale brown columnar like crystal formula $C_5H_5N_9$, triclinic, space group $P\bar{1}$(#2), a = 7.6069(6), b = 10.450(2), c = 5.7327(8) Å, α = 104.847(14), β = 109.680(8), γ = 96.967(13)°, U = 403.83(11) Å^3, Z = 2, D_c = 1.572 g cm^{-3}, R = 0.2333 was attached to a thin glass fibre and mounted on a Rigaku AFC7R diffractometer employing graphite monochromated CuKα radiation generated from a rotating anode. Cell constants were obtained from a least squares refinement against 25 reflections located between 92.40 and 104.20° 2θ. Data were collected at 293(2) Kelvin with $\omega - 2\theta$ scans to 135.28° 2θ. The intensities of 3 standard reflections measured every 150 reflections changed by −9.44 during the data collection and a correction was accordingly applied to the data. An empirical absorption correction based on azimuthal scans of three suitable reflections was also applied to the data. The data were corrected for Lorentz and polarisation effects.

Processing and calculations were undertaken with TEXSAN.[23] The structure was solved by direct methods with SIR97,[24] and extended and refined with SHELXL-97[25] using the TEXSAN interface. Anisotropic thermal parameters were refined for the 14 non-hydrogen atoms in the asymmetric unit of the structure model. A riding atom model was used for the hydrogens, which were placed at calculated positions with group thermal parameters. An ORTEP[26] depiction of the molecule is provided in Fig. 2.

Acknowledgements

Funding for part of this project by the Australian Research Council is acknowledged. Use of the ChemMatCARS Sector 15 at the Advanced Photon Source, was supported by the Australian Synchrotron Research Program, which is funded by the Commonwealth of Australia under the Major National Research Facilities Program. ChemMatCARS Sector 15 is also supported by the National Science Foundation/Department of Energy under grant numbers CHE9522232 and CHE0087817 and by the Illinois Board of Higher Education. The Advanced Photon Source is supported by the U.S. Department of Energy, Basic Energy Sciences, Office of Science, under Contract No. W-31–109-Eng-38.. The Australian Research Council for a Fellowship (DEH). The Lundbeck Foundation for post-doctoral funding (JRG). The Australian Centre for Advanced Computing and Communications (AC3) for computing resources.

References

1 N. Armstrong and E. Gouaux, *Neuron*, 2000, **28**, 165.
2 R. N. Butler, *Adv. Heterocyclic Chem.*, 1977, **21**, 323.
3 E. Cubero, M. Orozco and F. J. Luque, *J. Am. Chem. Soc.*, 1998, **120**, 4723.
4 H. A. Dabbagh and W. Lwowski, *J. Org. Chem.*, 2000, **65**, 7284.
5 V. P. Krivopalov, A. U. Denisov, U. V. Gaitlov and V. I. Mamatiuk, *Dokl. Akad. Nauk SSSR*, 1988, **300**, 115.
6 A. S. Katrusiak, M. Gdaniec and A. A. Katrusiak, *Pol. J. Chem.*, 1997, **71**, 488.
7 S. Baloniak and A. A. Katrusiak, *Pol. J. Chem.*, 1994, **68**, 683.
8 B. Stanovik and M. Tisler, *Tetrahedron*, 1969, **25**, 3313.
9 D-S. Choi, S. Huang, M. Huang, T. S. Barnard, R. D. Adams, J. M. Seminario and J. M. Tour, *J. Org. Chem.*, 1998, **63**, 2646.
10 P. Coad, R. A Coad, S. Clough, J. Hyepock, R. Salisbury and C. Wilkins, *J. Org. Chem.*, 1963, **28**, 218.
11 G. Vaccarella, Ph.D. Thesis, The University of Sydney, 1998.
12 G. Brauer, *Handbook of Preparative Inorganic Chemistry*, Academic Press, New York, 1963, 2nd edition, vol. 1, p. 534.
13 S. B. Harold and C. G. Seegmiller, *Inorg. Synth.*, 1946, **2**, 151.
14 R. N. Castle, *The Chemistry of heterocyclic compounds*, John Wiley & Sons, New York, 1973, vol. 27, part F, p. 893.
15 L. Golic, I. Leban, B. Stanovnik and M. Tisler, *Acta Crystallogr. Sect. B: Struct. Crystallogr. Cryst. Chem.*, 1978, **34**, 1136.
16 J. Ochterski, G. A. Petersson and J. A. Montgomery Jr., *J. Chem. Phys.*, 1996, **104**, 2598.
17 Jaguar 4.1, Schrödinger, Inc., Portland, OR, (2001).
18 J. R. Greenwood, H. R. Capper, R. D. Allan and G. A. R. Johnston, *Internet J. Chem.*, 1998, **1**, 21.
19 C. J. Cramer and D. G. Truhlar, *J. Am. Chem. Soc.*, 1993, **115**, 8810.
20 K. Frydenvang, J. R. Greenwood, S. B. Vogensen and L. Brehm, *Struct. Chem.*, 2002, **13**, 479.
21 M. J. Frisch, G. W. Trucks, H. B. Schlegel, G. E. Scuseria, M. A. Robb, J. R. Cheeseman, V. G. Zakrzewski, J. A. Montgomery, Jr., R. E. Stratmann, J. C. Burant, S. Dapprich, J. M. Millam, A. D. Daniels, K. N. Kudin, M. C. Strain, O. Farkas, J. Tomasi, V. Barone, M. Cossi, R. Cammi, B. Mennucci, C. Pomelli, C. Adamo, S. Clifford, J. Ochterski, G. A. Petersson, P. Y. Ayala, Q. Cui, K. Morokuma, D. K. Malick, A. D. Rabuck, K. Raghavachari, J. B. Foresman, J. Cioslowski, J. V. Ortiz, B. B. Stefanov, G. Liu, A. Liashenko, P. Piskorz, I. Komaromi, R. Gomperts, R. L. Martin, D. J. Fox, T. Keith, M. A. Al-Laham, C. Y. Peng, A. Nanayakkara, C. Gonzalez, M. Challacombe, P. M. W. Gill, B. G. Johnson, W. Chen, M. W. Wong, J. L. Andres, M. Head-Gordon, E. S. Replogle and J. A. Pople, GAUSSIAN 98 (Revision A.7), Gaussian, Inc., Pittsburgh, PA, 1998.
22 B. N. Ravi and R. J. Wells, *Aust. J. Chem.*, 1982, **35**, 129.
23 TEXSAN: Crystal Structure Analysis Package, Molecular Structure Corporation1985 & 1992.
24 A. Altomare, M. Cascarano, C. Giacovazzo and A. Guagliardi, *J. Appl. Crystallogr.*, 1993, **26**, 343.
25 G. M. Sheldrick, SHELXL97. Program for crystal structure refinement. University of Göttingen, Germany, 1997.
26 C. K. Johnson, ORTEPII. Report ORNL-5138. Oak Ridge National Laboratory, Oak Ridge, Tennessee, 1976.